

## Coinfecting Prion Strains Compete for a Limiting Cellular Resource<sup>∇†</sup>

Ronald A. Shikiya,<sup>1</sup> Jacob I. Ayers,<sup>1</sup> Charles R. Schutt,<sup>1</sup> Anthony E. Kincaid,<sup>1,2</sup> and Jason C. Bartz<sup>1\*</sup>

*Departments of Medical Microbiology and Immunology<sup>1</sup> and Physical Therapy,<sup>2</sup> Creighton University, Omaha, Nebraska 68178*

Received 2 February 2010/Accepted 4 March 2010

**Prion strain interference can influence the emergence of a dominant strain from a mixture; however, the mechanisms underlying prion strain interference are poorly understood. In our model of strain interference, inoculation of the sciatic nerve with the drowsy (DY) strain of the transmissible mink encephalopathy (TME) agent prior to superinfection with the hyper (HY) strain of TME can completely block HY TME from causing disease. We show here that the deposition of PrP<sup>Sc</sup>, in the absence of neuronal loss or spongiform change, in the central nervous system corresponds with the ability of DY TME to block HY TME infection. This suggests that DY TME agent-induced damage is not responsible for strain interference but rather prions compete for a cellular resource. We show that protein misfolding cyclic amplification (PMCA) of DY and HY TME maintains the strain-specific properties of PrP<sup>Sc</sup> and replicates infectious agent and that DY TME can interfere, or completely block, the emergence of HY TME. DY PrP<sup>Sc</sup> does not convert all of the available PrP<sup>C</sup> to PrP<sup>Sc</sup> in PMCA, suggesting the mechanism of prion strain interference is due to the sequestering of PrP<sup>C</sup> and/or other cellular components required for prion conversion. The emergence of HY TME in PMCA was controlled by the initial ratio of the TME agents. A higher ratio of DY to HY TME agent is required for complete blockage of HY TME in PMCA compared to several previous *in vivo* studies, suggesting that HY TME persists in animals coinfecting with the two strains. This was confirmed by PMCA detection of HY PrP<sup>Sc</sup> in animals where DY TME had completely blocked HY TME from causing disease.**

Prions are infectious agents of animals, including humans, which are comprised of PrP<sup>Sc</sup>, a misfolded isoform of the noninfectious host encoded protein PrP<sup>C</sup> (17, 24, 50, 63). Prion diseases of humans are unique neurodegenerative disorders in that they can have either a sporadic, familial, or infectious etiology. Prions cause disease in economically important domestic and wild animal species such as bovine spongiform encephalopathy in cattle and chronic wasting disease in wild and captive cervids (20, 62). Prion diseases can be zoonotic as illustrated by the transmission of bovine spongiform encephalopathy to humans that resulted in the emergence of variant Creutzfeldt-Jacob disease (14, 19, 22, 23, 46, 61, 68). Prion diseases are inevitably fatal and there are currently no effective treatments (21).

Prion strains are defined by a characteristic set of features that breed true upon experimental passage (33, 34). Strain-specific differences have been identified in incubation period, clinical signs, agent distribution, overdominance, host range, neuropathology, and biochemical properties of PrP<sup>Sc</sup> (5, 10, 11, 13, 28, 34, 42, 44). Strain-specific conformations of PrP<sup>Sc</sup> are hypothesized to encode prion strain diversity; however, it is not understood how these differences result in the distinct strain properties (11, 19, 40, 47, 59, 66).

Prion strain interference may be involved in the emergence of a dominant strain from a mixture as could occur during prion adaptation to a new host species or during prion evolution (4, 36, 43, 48, 56). In the natural prion diseases, there are

examples where an individual host may be infected with more than one prion strain (15, 25, 55, 57, 58). Experimentally, coinfection or superinfection of prion strains can result in interference where a blocking, long incubation period strain extends the incubation period or completely blocks a superinfecting, short incubation period strain from causing disease (26, 27). Prion interference has been described in experimental studies of mice and hamsters infected with a wide variety of prion strains and routes of inoculation, suggesting it may be a common property of prion disease (3, 27, 52, 53, 60).

It has been proposed that prion strains compete for a shared “replication site”; however, mechanistic details are not known, and it is unclear whether the blocking strain destroys or occupies the replication sites required for the superinfecting strain (28). The transport to and relative onset of replication of interfering strains in a common population of neurons is an important factor that can determine which strain will emerge (8). In the present study, we sought to determine whether the blocking strain disables transport and spread of the superinfecting strain or whether prion interference is due to competition for a cellular resource.

### MATERIALS AND METHODS

**Prion strains.** The hyper (HY) and drowsy (DY) strains of hamster-adapted transmissible mink encephalopathy (TME) were used in the present study (12). Both strains of TME were biologically cloned in hamsters by intracerebral (i.c.) passage of the isolate at the minimum infecting dose three times (4). The titer for each biologically cloned TME strain was determined by endpoint dilution of brain homogenate from terminally ill animals. The titers of HY TME and DY TME agents were 10<sup>9.3</sup> i.c. 50% lethal doses (LD<sub>50</sub>) and 10<sup>7.7</sup> i.c. LD<sub>50</sub> per g of brain, respectively (45).

**Animal inoculations.** All procedures involving animals were approved by the Creighton University Institutional Animal Care and Use Committee and comply with the *Guide for the Care and Use of Laboratory Animals*. Male Syrian golden hamsters (Harlan-Sprague-Dawley, Indianapolis, IN) were used, and sciatic nerve inoculations were performed as previously described (7). Briefly, animals

\* Corresponding author. Mailing address: Department of Medical Microbiology and Immunology, 2500 California Plaza, Omaha, NE 68178. Phone: (402) 280-1811. Fax: (402) 280-1875. E-mail: jbartz@creighton.edu.

<sup>∇</sup> Published ahead of print on 17 March 2010.

<sup>†</sup> The authors have paid a fee to allow immediate free access to this article.

were anesthetized with isoflurane, the right sciatic nerve was exposed, and a 30-gauge needle was inserted into the nerve and reciprocated 10 times prior to injection with either 1  $\mu$ l of a 1% (wt/vol) brain homogenate containing  $10^{2-7}$  i.c. LD<sub>50</sub> of the DY TME agent or a mock-infected homogenate. After injection, the wound was closed by using surgical staples and the animals allowed to recover from anesthesia. Animals were i.c. inoculated with 25  $\mu$ l of a 1% (wt/vol) brain homogenate as described previously (45). Hamsters were observed three times per week for the onset of clinical signs, and the incubation period was calculated as the number of days between inoculation and the onset of clinical disease (45).

**Tissue collection.** For experiments involving immunohistochemistry, retrograde tracer analysis, and neuronal cell counting, prion-infected and age-matched mock-infected hamsters were anesthetized with isoflurane and transcardially perfused with 50 ml of 0.01 M Dulbecco phosphate-buffered saline, followed by 75 ml of McLean's paraformaldehyde-lysine-periodate (PLP) fixative (69). The lumbar spinal cord (L4 to L6) and sciatic nerve were immediately removed and immersed in PLP for 5 to 7 h at room temperature prior to paraffin processing or immersed in 20% (wt/vol) sucrose for 24 h at 4°C prior to frozen sectioning (7). For protein misfolding cyclic amplification experiments, uninfected hamsters were anesthetized with isoflurane and transcardially perfused with 75 ml of ice-cold phosphate-buffered saline containing 5 mM EDTA (pH 7.4) (17). Brain tissue was immediately collected, frozen on dry ice, and stored at -80°C until use.

**Immunohistochemistry.** Immunohistochemistry was performed as previously described (2). Briefly, 7- $\mu$ m tissue sections were deparaffinized and incubated in 95% formic acid (Sigma-Aldrich, St. Louis, MO) for 20 min at room temperature. Endogenous peroxidase activity was blocked using 0.3% H<sub>2</sub>O<sub>2</sub> in methanol for 20 min at room temperature. Nonspecific staining was blocked with 10% normal horse serum (Vector Laboratories, Burlingame, CA) in Tris-buffered saline for 30 min at room temperature. The sections were incubated in either the anti-PrP monoclonal antibody 3F4 (1:600; Chemicon, Billerica, MA), anti-glial fibrillary acidic protein (GFAP; 1:16,000; Dako, Carpinteria, CA), anti-ionized calcium-binding adaptor molecule 1 (Iba-1; 1:500; Abcam, Cambridge, MA), or anti-synaptophysin (1:400; Dako; Carpinteria, CA) at 4°C overnight. The sections were incubated in either a biotinylated horse anti-mouse, anti-goat, or anti-rabbit immunoglobulin G conjugate and subsequently incubated in ABC solution (Elite kit; Vector Laboratories, Burlingame, CA). Sections were developed using 0.05% (wt/vol) 3,3'-diaminobenzidine (Sigma-Aldrich) in Tris-buffered saline containing 0.0015% H<sub>2</sub>O<sub>2</sub> and counterstained with hematoxylin (Richard Allen Scientific, Kalamazoo, MI). Light microscopy was performed by using a Nikon i80 microscope (Nikon, Melville, NY), and images were captured and processed as described previously (2). Tissue sections were analyzed at a sampling interval of no greater than 126  $\mu$ m.

**Retrograde tracer injection and analysis.** At 120 days after right sciatic nerve inoculation, the DY TME agent-infected and age-matched mock-infected hamsters were anesthetized with isoflurane prior to injection of the right sciatic nerve with 2  $\mu$ l of a 10% (wt/vol) solution of 10,000-molecular-weight lysine-fixable dextran conjugated to Alexa Fluor 568 using a 30-gauge needle. The animals were sacrificed 72 h postinjection, and 30- $\mu$ m tissue sections of sucrose impregnated lumbar spinal cord were cut by using a cryostat (Leica, Bannockburn, IL). Fluorescence microscopy was performed by using a Nikon i80 microscope (Nikon, Melville, NY). Images were captured by using a DigiFire camera and ImageSys digital imaging software (Soft Imaging Systems, Lakewood, CO).

**Nissl staining and neuronal cell counting.** DY TME agent-infected ( $n = 4$ ) or age-matched mock-infected ( $n = 4$ ) hamsters were sacrificed at 120 days after sciatic nerve inoculation, and sucrose-impregnated L4-L6 lumbar spinal cord sections were cut at 30  $\mu$ m using a cryostat (Leica). The free-floating sections were stained with cresyl violet (Sigma-Aldrich), mounted on glass slides, air-dried overnight, and cover slipped in mounting media (Richard Allen Scientific). Ventral motor neurons (VMNs) in lamina IX of the spinal cord were identified based on characteristic morphological features (8). Student *t* test was used to compare the groups using the Prism 4.0 (for Macintosh) software program (GraphPad Software, Inc., San Diego, CA).

**Protein misfolding cyclic amplification.** Hamster brain was homogenized to 10% (wt/vol) in ice-cold conversion buffer (phosphate-buffered saline [pH 7.4] containing 5 mM EDTA, 1% [vol/vol] Triton X-100, and Complete protease inhibitor tablet [Roche Diagnostics, Mannheim, Germany]) using a Tenbroeck tissue grinder (Vineland, NJ). The brain homogenate was centrifuged at 500  $\times$  *g* for 30 s. The supernatant was collected and stored at -80°C. Protein misfolding cyclic amplification (PMCA) was performed with a Misonix 3000 sonicator (Farmingdale, NY). The sonicator output was set at level 6 with an average output of 156 W during each sonication cycle. The homogenates in conversion buffer were placed into polypropylene PCR tubes and subjected to one round of PMCA. A PMCA round consisted of 144 cycles of a 5-s sonication, followed by

a 10-min incubation at 37°C. Before each PMCA round, an aliquot was placed at -80°C as an unsonicated control. After the first round of PMCA, an aliquot of the sonicated sample was added to fresh 10% (wt/vol) uninfected brain homogenate in conversion buffer and subjected to a second round of PMCA. The ratio of sonicated sample to uninfected brain homogenate was 1:20 for HY TME-seeded reactions. For DY TME-seeded reactions, the ratio of sonicated to uninfected brain homogenate was 1:20 for the first round, 1:10 for the second round, and 1:2 for the remaining rounds of PMCA. In PMCA samples that contained both DY and HY TME agents the ratio of sonicated to uninfected brain homogenate was 1:2. Samples containing uninfected brain homogenate in conversion buffer were included in every round of PMCA as a negative control.

**Western blot analysis.** Western blot detection of PrP<sup>Sc</sup> from brain homogenate was performed as described previously (8). Briefly, brain homogenate (5% [wt/vol]) is digested with proteinase K (PK) at a final concentration of 1 U/ml (Roche Diagnostics Corp., Indianapolis, IN) at 37°C for 30 min. The PK digestion is terminated by incubating the samples at 100°C for 10 min. For deglycosylation, the PK-treated sample was digested by using PNGase F (New England Biolabs, Ipswich, MA) according to the manufacturer's instructions. The samples were size fractionated with 4-12% bis-Tris-acrylamide SDS-PAGE and transferred to a polyvinylidene difluoride membrane (NuPage; Invitrogen, Carlsbad, CA). The membrane was blocked with 5% nonfat dry milk (Bio-Rad Laboratories, Hercules, CA) for 30 min. Hamster prion protein was detected using the mouse monoclonal anti-PrP antibody 3F4 (1:10,000; Chemicon, Temecula, CA). The Western blot was developed with Pierce Supersignal West Femto maximum sensitivity substrate, according to the manufacturer's instructions (Pierce, Rockford, IL), and imaged on a Kodak 4000R imaging station (Kodak, Rochester, NY). The quantification of PrP<sup>Sc</sup> abundance and the comparison of PrP<sup>Sc</sup> abundance between samples were performed using Kodak Molecular Imaging Software v.5.0.1.27 (New Haven, CT) as previously described (8).

## RESULTS

**Absence of neuropathological changes after DY TME agent infection when HY TME superinfection is blocked.** Inoculation of the DY TME agent 120 days prior to superinfection with the HY TME agent results in DY TME completely blocking HY TME from causing disease (8, 60). The location of strain interference in this model system is the VMNs in the lumbar spinal cord, ipsilateral to the side of sciatic nerve inoculation (8).

To test the hypothesis that DY TME infection induced a deficit in axonal transport, the sciatic nerve was injected with a retrograde tracer at 120 days postinoculation with brain homogenates from either mock-infected or DY TME agent-infected hamsters (Fig. 1A and B, respectively). The number of dextran-positive VMNs in the mock-infected ( $n = 4$ ) and DY TME-infected ( $n = 5$ ) groups did not significantly ( $P > 0.05$ ) differ (Fig. 1C), suggesting that the DY TME agent does not inhibit axonal transport from the site of inoculation in the sciatic nerve to VMNs in the lumbar spinal cord.

To test the hypothesis that DY TME agent infection-induced VMN cell death is responsible for interference, the number of VMNs was counted on Nissl-stained sections from hamsters that were inoculated in the sciatic nerve with either uninfected or DY TME agent-infected brain homogenate at 120 days postinfection. In the DY TME agent-infected animals, we compared the number of VMNs between the ipsilateral and contralateral sides of inoculation. The ipsilateral population of VMNs have been shown to completely block superinfection of HY TME, while the contralateral population of VMNs can completely allow HY TME infection (8); therefore, this internal control ensures that similar populations of VMNs were compared. The number of VMNs ipsilateral to the side of inoculation (Fig. 1E) were similar ( $P > 0.05$ ) (Fig. 1F) to the number of VMNs contralateral to the side of inoculation

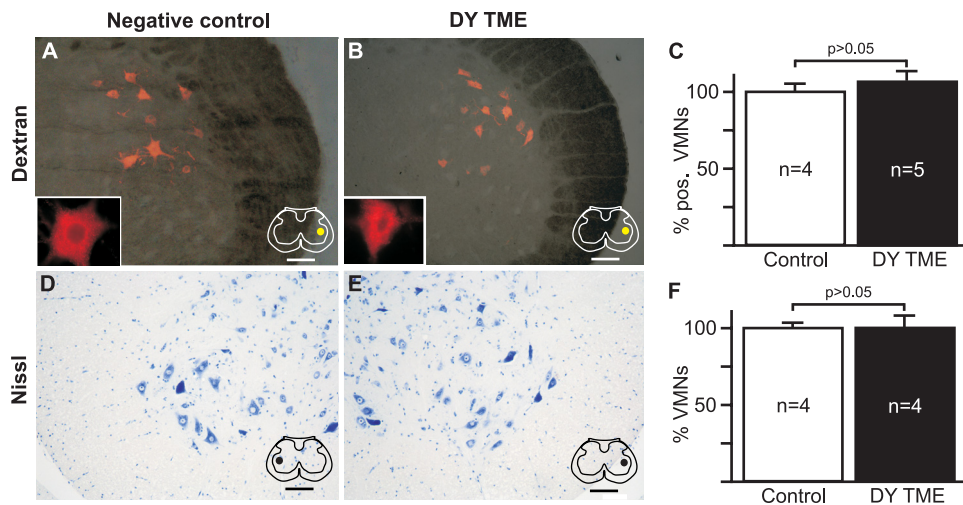


FIG. 1. The DY TME agent does not significantly inhibit retrograde transport or cause death of VMNs. Lumbar spinal cord sections from hamsters that were injected in the sciatic nerve with dextran conjugated to Alexa Fluor 568 at 120 days after sciatic nerve inoculation with either an uninfected brain homogenate (A) or DY TME agent (B). Insets in panels A and B depict dextran-positive ventral motor neurons. (C) The number of VMNs containing dextran in the lumbar spinal cord from the DY TME agent infected did not differ significantly ( $P > 0.05$ ) compared to the negative control animals. The number of VMNs in Nissl-stained sections of lumbar spinal cord collected from hamsters at 120 days after sciatic nerve inoculation with the DY TME agent contralateral (D) or ipsilateral (E) to the side of inoculation did not significantly ( $P > 0.05$ ) differ (F). The yellow regions in the schematic insets depict the location of the spinal cord that were imaged. Scale bar, 100  $\mu\text{m}$ .

(Fig. 1D). In addition, the number of VMNs in mock-infected ( $n = 4$ ) and DY TME-infected ( $n = 4$ ) were similar ( $P > 0.05$ ) (data not shown). These data suggest that the DY TME agent does not cause death of VMNs at 120 days postinfection.

Thus, it appears that the superinfecting HY TME agent can be transported retrogradely to viable VMNs after DY TME agent inoculation. Since HY PrP<sup>Sc</sup> is initially detected in VMNs at 14 days postinfection in animals inoculated in the sciatic nerve with the HY TME agent (2), we examined lumbar spinal cord for neuropathological changes at 134 days (120 plus 14 days) after DY TME agent infection. No spongiform degeneration, reactive astrocytosis, microgliosis, or loss of synaptic density was detected ipsilateral or contralateral to the side of inoculation (Fig. 2 panels A, B, I, J, M, N, Q, and R). Deposition of DY PrP<sup>Sc</sup> was restricted to the ipsilateral lumbar spinal cord and was not detected in the contralateral lumbar spinal cord (Fig. 2E and F). In the same region of the lumbar spinal cord, spongiform degeneration, PrP<sup>Sc</sup> deposition, reactive astrocytosis, and microgliosis were observed, but synaptophysin immunoreactivity was unchanged at DY TME clinical disease (Fig. 2C, G, K, O, and S). Neither spongiform degeneration, PrP<sup>Sc</sup> deposition, reactive astrocytosis, microgliosis, nor a loss of synaptophysin immunoreactivity were observed in mock-infected animals (Fig. 2D, H, L, P, and T). These data are consistent with PrP<sup>Sc</sup> deposition as the main observable neuropathological feature that correlates with the ability of the DY TME agent to block superinfecting HY TME agent from causing disease.

**Strain-specific characteristics of HY and DY PrP<sup>Sc</sup> are recapitulated by PMCA.** Brain homogenates that were prepared from hamsters infected with biologically cloned HY TME or DY TME agents or from uninfected controls were subjected to PMCA. After one round of PMCA, the abundance of PrP<sup>Sc</sup>

was greater following PMCA compared to the unsonicated controls for both HY and DY TME seeded reactions (Fig. 3A, lanes 5 to 8, and panel B). The abundance of PrP<sup>Sc</sup> after one round of PMCA was greater in HY TME-seeded reactions compared to DY TME-seeded reactions (Fig. 3B), suggesting HY TME amplifies more efficiently. In the uninfected-homogenate negative control PMCA reactions, PrP<sup>Sc</sup> was not detected (Fig. 3A, lanes 3 to 4, and panel B). Brain-derived PK-digested PrP<sup>Sc</sup> from DY TME-infected animals migrates 1 to 2 kDa faster than PrP<sup>Sc</sup> from HY TME-infected animals (Fig. 3C, lanes 1 and 2) (11). The strain-specific migration properties of HY and DY PrP<sup>Sc</sup> are maintained after 10 rounds of serial PMCA (Fig. 3C, lanes 4 and 5). Digestion of brain-derived and PMCA-generated HY and DY PrP<sup>Sc</sup> with PNGase results in the expected 1- to 2-kDa strain-specific difference in PrP<sup>Sc</sup> migration (Fig. 3C, lanes 7 to 10).

**PMCA-generated PrP<sup>Sc</sup> is infectious.** The PMCA reactions were initially seeded with 5  $\mu\text{l}$  of a 10% (wt/vol) brain homogenate from either HY TME- or DY TME-infected hamsters that contained  $5 \times 10^{5.3}$  or  $5 \times 10^{3.7}$  i.c. LD<sub>50</sub>, respectively. After 10 rounds of serial PMCA and a final 1:10 dilution prior to inoculation, the initial HY TME and DY TME agent seeds are diluted  $10^{-14}$ - and  $10^{-7}$ -fold, respectively, which dilutes the initial TME seed beyond the limit of detection of animal bioassay (4, 6, 45). All of the hamsters i.c. inoculated with a 1% (wt/vol)/HY TME brain homogenate ( $n = 5$ ) or the tenth serial PMCA round of HY TME-seeded reactions ( $n = 5$ ) developed clinical signs of hyper excitability and ataxia at  $61 \pm 3$  (Fig. 3D, solid diamonds) and  $83 \pm 3$  days postinfection (Fig. 3D, solid squares), respectively, with a PrP<sup>Sc</sup> migration pattern that is consistent with HY TME agent infection (data not shown). All ( $n = 5$ ) of the hamsters inoculated with the 1% (wt/vol) DY TME brain homogenate developed clinical signs of progressive lethargy at  $172 \pm 3$  days postinfection (Fig. 3D, open dia-

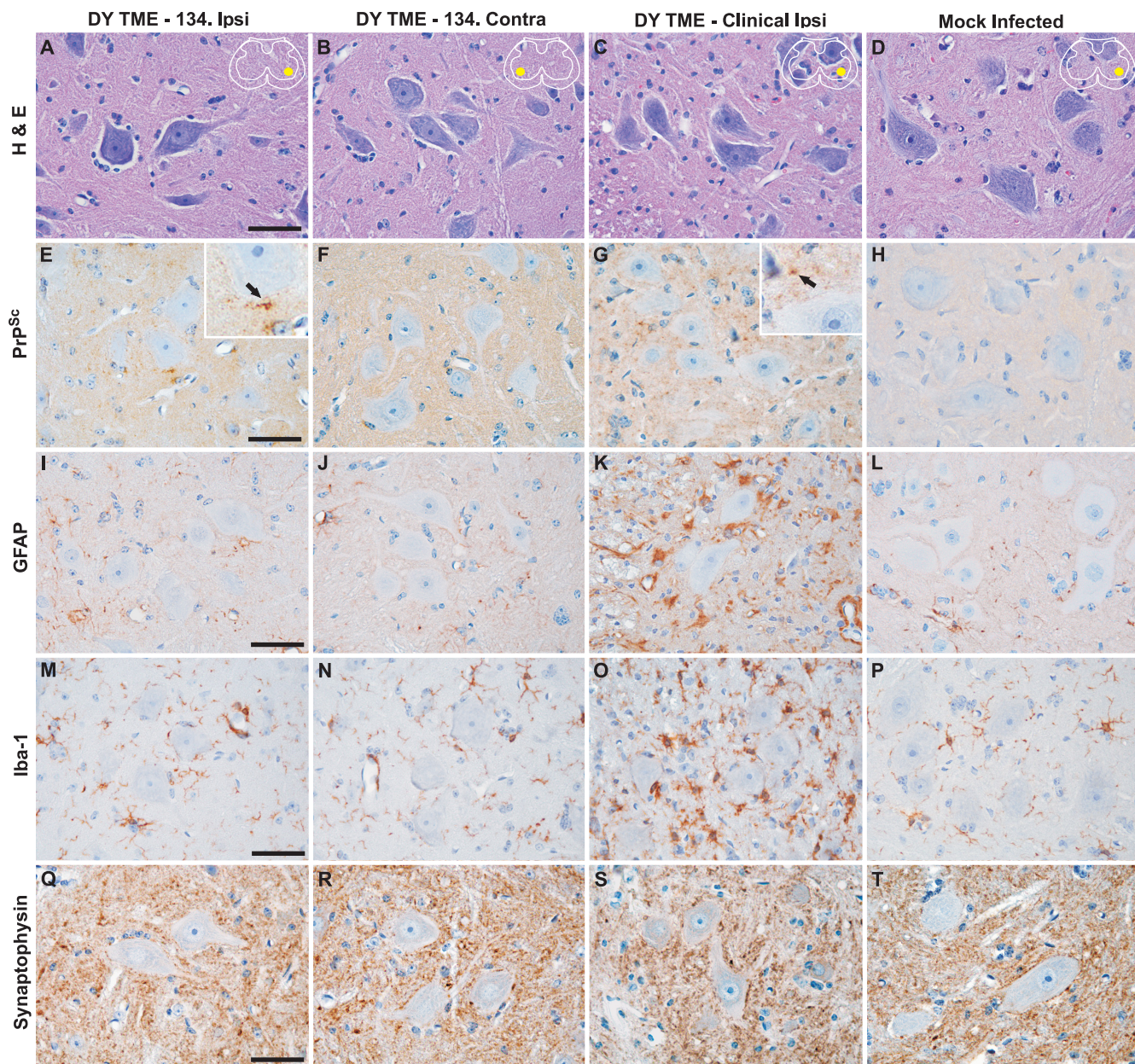


FIG. 2. PrP<sup>Sc</sup> deposition is present in the absence of spongiform degeneration, astrocytosis, microgliosis, and synaptic loss in the lumbar spinal cord at 134 days after DY TME agent inoculation. Hamsters were inoculated in the sciatic nerve with either the DY TME agent or uninfected (Mock) brain homogenate and lumbar spinal cord was collected at 134 days postinfection or at clinical disease. Lumbar spinal cord sections were stained either with hematoxylin and eosin (H&E) or immunohistochemistry was performed using antibodies directed against PrP<sup>Sc</sup>, glial fibrillary acidic protein (GFAP), ionized calcium-binding adaptor molecule 1 (Iba-1) or synaptophysin. The yellow regions in the schematic insets depict the location of the brain that were imaged for each column. Arrows indicate PrP<sup>Sc</sup> deposits in the panel E and G insets. Scale bar, 50  $\mu$ m.

monds). Five hamsters were i.c. inoculated with the tenth serial PMCA round of DY TME-seeded reactions. One intercurrent death occurred at 187 days postinfection, and the remaining four hamsters developed clinical signs of progressive lethargy at  $205 \pm 11$  days postinfection (Fig. 3D, open squares). All of these animals, including the intercurrent death, had PrP<sup>Sc</sup> with a migration pattern consistent with DY TME agent infection (data not shown). Hamsters i.c. inoculated with 10 serial PMCA rounds of uninfected brain homogenate (Fig. 3D, solid

circles) remain clinically unaffected at greater than 300 days postinfection.

**Limits of HY PrP<sup>Sc</sup> detection using PMCA.** Brain homogenate from HY TME-infected hamsters was 10-fold serial diluted into uninfected hamster brain homogenate and these samples were subjected to 10 rounds of serial PMCA. Western blot was performed after each round of PMCA to determine whether PrP<sup>Sc</sup> was present. After one round of PMCA, PrP<sup>Sc</sup> was detected in PMCA reactions that were initially seeded with

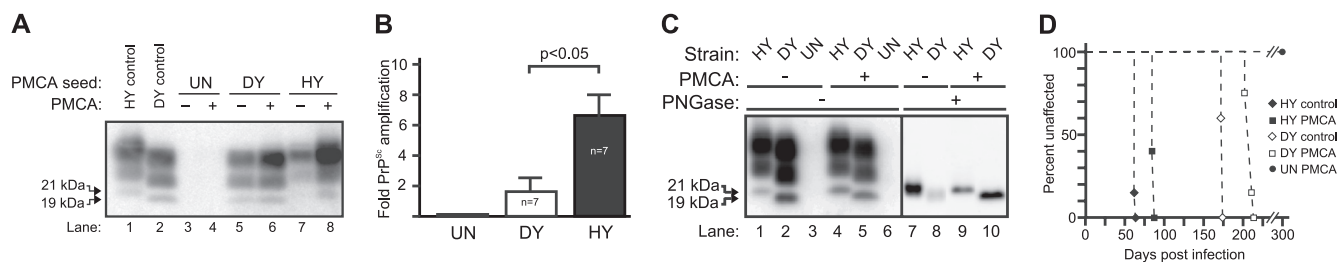


FIG. 3. Strain-specific characteristics of HY and DY PrP<sup>Sc</sup> are recapitulated by PMCA. (A) PMCA reactions were seeded with uninfected (UN), DY TME-infected (DY), or HY TME-infected brain homogenates (HY) and one round of PMCA resulted in detection of PK digestion-resistant PrP<sup>Sc</sup> in the DY TME- and HY TME-seeded reactions but not in the negative control uninfected seeded reactions. (B) HY PrP<sup>Sc</sup> accumulated to a higher abundance compared to DY PrP<sup>Sc</sup>, suggesting that HY TME amplifies more efficiently than DY PrP<sup>Sc</sup>. (C) Western blot analysis of PK-digested brain homogenates from HY TME (HY), DY TME (DY), or uninfected hamster (UN) before (lanes 1 to 3, 7, and 8) or after PMCA (lanes 4 to 6, 9, and 10) treated without (1–6) or with (7–10) PNGase indicates that the strain-specific migration of HY TME and DY TME PrP<sup>Sc</sup> is maintained after PMCA. The migration of the 19- and 21-kDa unglycosylated PrP<sup>Sc</sup> polypeptide is indicated on the left of the panel. (D) Survival of Syrian hamsters after i.c. inoculation of HY TME agent ( $n = 5$ ,  $\blacklozenge$ ), DY TME agent ( $n = 5$ ,  $\diamond$ ), or the tenth serial PMCA round of HY TME ( $n = 5$ ,  $\blacksquare$ ), DY TME ( $n = 4$ ,  $\square$ ), or mock ( $n = 5$ ,  $\bullet$ )-seeded reactions.

500 to  $5 \times 10^{-2}$   $\mu\text{g}$  brain equivalents of HY TME but was not detected in PMCA reactions seeded with lower amounts ( $5 \times 10^{-3}$  to  $5 \times 10^{-9}$ ) of HY TME (Table 1). After each subsequent round of serial PMCA, PrP<sup>Sc</sup> was detected in samples that contained decreasingly smaller amounts of initial seed of HY TME brain homogenate (Table 1). After the tenth round of serial PMCA HY PrP<sup>Sc</sup> was detected in samples that initially contained  $5 \times 10^{-8}$   $\mu\text{g}$  eq of HY TME (Table 1). HY PrP<sup>Sc</sup> was not detected in PMCA reactions that contained less than  $5 \times 10^{-9}$   $\mu\text{g}$  eq of HY TME or in uninfected brain homogenate-negative control samples through 10 rounds of serial PMCA (Table 1).

**HY and DY TME PMCA strain interference.** To investigate whether HY and DY TME interference could occur in a cell-free system, 500  $\mu\text{g}$  eq of DY TME brain homogenate was mixed with decreasing amounts of HY TME brain homogenate and the mixture was subjected to 10 rounds of serial PMCA. For each experiment, a HY TME and a DY TME brain homogenate-only sample was included as a positive control and a sample of uninfected hamster brain homogenate was included as a negative control. Western blot of the PMCA reactions determined the migration properties of the amplified PrP<sup>Sc</sup> after each round of PMCA. Both the initial ratio of DY and HY TME agent and the number of rounds of PMCA influenced which strain emerged based on migration properties of PrP<sup>Sc</sup> (Table 2). For example, after four rounds of PMCA a

ratio of HY TME to DY TME brain homogenate ranging from 1:1 to 1:1,000 resulted in the detection of HY PrP<sup>Sc</sup> (Fig. 4A, lanes 3 to 6, and Table 2) and when DY TME was present in  $>10,000$ -fold excess to HY TME, DY PrP<sup>Sc</sup> was detected (Fig. 4A, lanes 7 to 11, and Table 2). When the ratio of HY to DY TME was kept constant at a 1:10,000, DY PrP<sup>Sc</sup> was detected from the first through the eighth round of PMCA (Fig. 4B, lanes 3 to 10, and Table 2) and HY PrP<sup>Sc</sup> emerged at the ninth round and was maintained upon subsequent rounds of PMCA (Fig. 4B, lanes 11 to 12, and Table 2). Overall, there was an inverse relationship between the initial abundance of HY TME present in the sample and the number of rounds of PMCA required for HY PrP<sup>Sc</sup> to emerge (Table 2). When the ratio of HY TME to DY TME was  $<1:100,000$ , HY PrP<sup>Sc</sup> failed to emerge after 15 rounds of PMCA (Table 2 and data not shown); however, PMCA reactions seeded with this same dose of HY TME ( $5 \times 10^{-3}$   $\mu\text{g}$  eq) alone resulted in detection of HY PrP<sup>Sc</sup> by the second round of PMCA (Table 1).

**Persistence of HY TME in animals coinfecting with the DY and HY TME agents.** The PMCA strain interference results indicated that a higher ratio of DY TME agent to HY TME agent was required to completely block HY PrP<sup>Sc</sup> from emerging compared to *in vivo* studies (4, 8, 60). This suggests that the HY TME agent persists in the central nervous systems (CNS) of coinfecting animals in conditions where the DY TME agent is able to completely block HY TME from causing disease. To

TABLE 1. PMCA detection limits of HY TME<sup>a</sup>

PMCA round	HY TME brain equivalents ( $\mu\text{g}$ )												
	500	50	5	$5 \times 10^{-1}$	$5 \times 10^{-2}$	$5 \times 10^{-3}$	$5 \times 10^{-4}$	$5 \times 10^{-5}$	$5 \times 10^{-6}$	$5 \times 10^{-7}$	$5 \times 10^{-8}$	$5 \times 10^{-9}$	Mock
1	+	+	+	+	+	-	-	-	-	-	-	-	-
2	+	+	+	+	+	+	-	-	-	-	-	-	-
3	+	+	+	+	+	+	+	-	-	-	-	-	-
4	+	+	+	+	+	+	+	+	+	+	-	-	-
5	+	+	+	+	+	+	+	+	+	+	-	-	-
6	+	+	+	+	+	+	+	+	+	+	+	-	-
7	+	+	+	+	+	+	+	+	+	+	+	-	-
8	+	+	+	+	+	+	+	+	+	+	+	-	-
9	+	+	+	+	+	+	+	+	+	+	+	-	-
10	+	+	+	+	+	+	+	+	+	+	+	-	-

<sup>a</sup> +, Detectable PrP<sup>Sc</sup> amplification; -, undetectable PrP<sup>Sc</sup> amplification.

TABLE 2. PMCA interference of DY and HY TME

PMCA round	Initial PMCA reaction sample starting contents <sup>a</sup>								
	500 µg eq. HY TME	500 µg eq. DY TME	Mock	500 µg eq. HY TME + 500 µg eq. DY TME	50 µg eq. HY TME + 500 µg eq. DY TME	5 µg eq. HY TME + 500 µg eq. DY TME	5 × 10 <sup>-1</sup> µg eq. HY TME + 500 µg eq. DY TME	5 × 10 <sup>-2</sup> µg eq. HY TME + 500 µg eq. DY TME	5 × 10 <sup>-3</sup> µg eq. HY TME + 500 µg eq. DY TME
1	HY	DY	-	HY/DY	DY	DY	DY	DY	DY
2	HY	DY	-	HY	HY	DY	DY	DY	DY
3	HY	DY	-	HY	HY	DY	DY	DY	DY
4	HY	DY	-	HY	HY	HY	HY	DY	DY
5	HY	DY	-	HY	HY	HY	HY	DY	DY
6	HY	DY	-	ND <sup>4</sup>	ND	ND	ND	DY	DY
7	HY	DY	-	ND	ND	ND	ND	DY	DY
8	HY	DY	-	ND	ND	ND	ND	DY	DY
9	HY	DY	-	ND	ND	ND	ND	HY	DY
10	HY	DY	-	ND	ND	ND	ND	HY	DY

<sup>a</sup> eq., equivalents; HY, PrP<sup>Sc</sup> with HY TME migration pattern; DY, PrP<sup>Sc</sup> with DY TME migration pattern; -, PrP<sup>Sc</sup> not detected; ND, not done.

investigate this possibility, we performed serial PMCA on archived brain homogenate from hamsters inoculated in the sciatic nerve with the DY TME agent 120 days prior to sciatic nerve superinfection with either HY TME, 263K, or hamster-adapted chronic wasting disease (HaCWD) agents (8, 60). Under these conditions the DY TME agent can completely block HY TME from causing disease, and Western blot analysis detects only DY PrP<sup>Sc</sup> (8, 60). PMCA of brain material from these animals resulted in PrP<sup>Sc</sup> that migrates similar to DY PrP<sup>Sc</sup> (Fig. 5, lanes 6 and 7) after the first and second rounds of serial PMCA. However, by the third round of serial

PMCA, the amplified PrP<sup>Sc</sup> migration is similar to HY TME, 263K, or HaCWD PrP<sup>Sc</sup>, and this migration pattern is maintained upon subsequent passage (Fig. 5, lanes 8 and 9, and data not shown). As controls, brain material from an uninfected (UN) hamster or from hamsters with terminal disease infected in the sciatic nerve with either the HY TME or the DY TME agent was subjected to four rounds of serial PMCA. This resulted in either a failure to detect PrP<sup>Sc</sup>, detection of HY PrP<sup>Sc</sup>, or detection DY PrP<sup>Sc</sup>, respectively (Fig. 5, lanes 3, 4, and 5).

DISCUSSION

The DY and HY TME agents are known to be retrogradely transynaptically transported within the CNS along the same four descending motor pathways after sciatic nerve inoculation (2). Interruption of these pathways would be expected to pre-

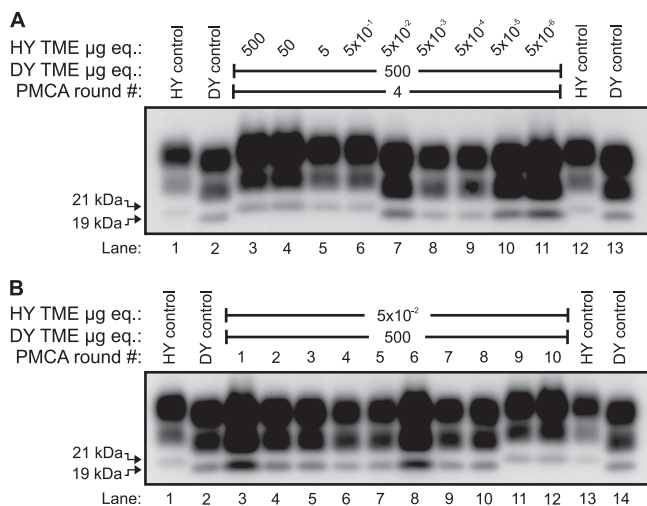


FIG. 4. Protein misfolding cyclic amplification strain interference. Known amounts of HY TME-infected and DY TME-infected brain homogenate were combined and added to PMCA reactions, and 10 rounds of serial PMCA were performed. (A) After four rounds of serial PMCA, Western blot analysis determined that PrP<sup>Sc</sup> migration was consistent with HY PrP<sup>Sc</sup> when the initial ratio of DY TME to HY TME brain homogenate ranged from 1:1 to 1:1,000, respectively (lanes 3 to 6) and was consistent with DY PrP<sup>Sc</sup> when the ratio of DY TME to HY TME brain homogenate was greater than 1:10,000 (lanes 7 to 11). (B) When the ratio of DY to HY TME brain homogenate was 1:10,000, the migration of PrP<sup>Sc</sup> was consistent with DY PrP<sup>Sc</sup> during the first eight rounds of serial PMCA (lanes 3 to 8) but then changed to a migration pattern consistent with HY PrP<sup>Sc</sup> during rounds 9 and 10 (lanes 11 to 12).

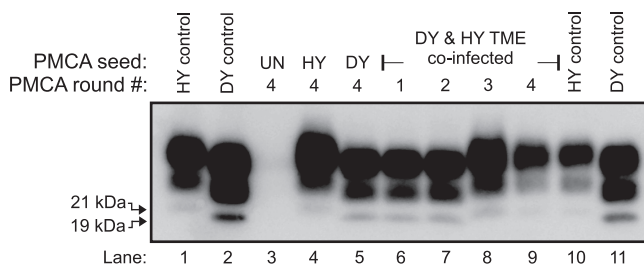


FIG. 5. Persistence of HY TME in animals coinfected with the DY TME and HY TME agents. Four rounds of serial PMCA was performed on brain homogenate from uninfected (UN) hamsters, hamsters infected with either the HY TME agent (HY) or the DY TME agent (DY), or hamsters infected under conditions where the DY TME agent completely blocks the HY TME agent from causing disease. Western blot analysis of PK-digested sample from the uninfected negative control PMCA indicated that it did not amplify PrP<sup>Sc</sup> (lane 3). The HY TME and DY TME positive control PMCA reactions amplified PrP<sup>Sc</sup> that maintained the 21- and 19-kDa strain-specific PrP<sup>Sc</sup> migration pattern (lanes 4 and 5, respectively). In the group of superinfected hamsters, one round of PMCA results in a 19-kDa PrP<sup>Sc</sup> migration pattern consistent with DY PrP<sup>Sc</sup> (compare lanes 5 and 6). After four rounds of serial PMCA, the PrP<sup>Sc</sup> migration pattern is consistent with HY PrP<sup>Sc</sup> (compare lanes 9 to 10). The migration of the 19- and 21-kDa unglycosylated PrP<sup>Sc</sup> polypeptide is indicated on the left of the panel.

vent the agent from reaching the clinical target areas and causing disease. In the first set of experiments we investigated whether the DY TME agent interfered with the transport or spread of the superinfected HY TME agent. At 120 days after DY TME agent infection, when it can completely block superinfected HY TME agent from causing disease, transport of dextran from the site of inoculation in the sciatic nerve to VMNs was not affected, suggesting that inhibition of axonal transport was not responsible for strain interference (Fig. 1) (8, 60). This result is consistent with the observation that in animals where DY TME agent extends the incubation period of HY TME, the initial detection of HY PrP<sup>Sc</sup> in the lumbar spinal cord is not delayed (8). In addition, while recent findings indicate that inhibition of axonal transport in prion-infected animals occurs, it is not observed prior to the onset of clinical signs consistent with the findings presented here (29, 30). The mechanism of axonal transport of PrP<sup>Sc</sup> is not known; therefore, we cannot exclude the possibility that dextran and PrP<sup>Sc</sup> use different transport mechanisms. However, in cell culture systems, the movements of dextran and PrP<sup>Sc</sup> are similar (49). We also examined whether DY TME agent-induced VMN death was responsible for strain interference. In this model system, DY TME agent-induced death of VMNs at 120 days postinfection would not be expected to affect progression of DY TME disease since it has transynaptically spread rostrally from VMNs to the brain stem by this time (2). Death of VMNs at 120 days after DY TME agent infection, however, would be expected to prevent HY TME from causing disease since VMNs are the first population of neurons in the CNS infected with HY TME after sciatic nerve inoculation (2). However, a reduction in the number of VMNs was not observed in DY TME-infected animals at time points postinfection, where it can completely block HY TME from causing disease (Fig. 1). Based on these observations, it is likely that the superinfected HY TME agent is able to reach a viable population of VMNs.

The only observable pathological change *in vivo* that correlates with the ability of DY TME to interfere with HY TME infection is the deposition of PrP<sup>Sc</sup> (Fig. 2). We did not observe a reactive astrocytosis, microgliosis, or spongiosis in the lumbar spinal cord at 134 days after DY TME infection (Fig. 2), which is consistent with the lack of evidence of VMN cell death (Fig. 1). These pathological changes were observed at clinical disease, indicating that they could occur in the lumbar spinal cord. The absence of pathology at preclinical time points indicated that they did not correlate with the ability of the DY TME agent to interfere with the HY TME agent. We also did not observe a reduction in synaptophysin immunoreactivity in the lumbar spinal cord in DY TME-infected animals, which suggests that synapses have not been lost at this time point postinfection (Fig. 2). Alternatively, we cannot exclude the possibility that other mechanisms of cell-to-cell spread of agent, such as exosomes and tunneling nanotubes, are inhibited and may contribute to the interference effect (1, 32, 37, 38, 67). The only pathology observed is the deposition of DY PrP<sup>Sc</sup> in lamina IX of the lumbar spinal cord ipsilateral, but not contralateral, to the side of sciatic nerve inoculation. Significantly, HY TME agent superinfection of the ipsilateral sciatic nerve results in complete blockage of HY TME disease, while superinfection of the contralateral sciatic nerve results in animals succumbing to HY TME infection (8). These data suggest that DY PrP<sup>Sc</sup> is

competing with HY PrP<sup>Sc</sup> for a limiting host resource that is not related to cellular damage induced by replication of the DY TME agent.

To investigate the hypothesis that strain interference is due to competition for a host resource, we examined whether prion strain interference could occur in a cell-free system. In the experiments reported here, PMCA of HY and DY TME maintained the strain-specific biochemical properties of PrP<sup>Sc</sup>, a finding consistent with previous studies (Fig. 3) (11, 16, 39). Inoculation of hamsters with the HY or DY TME PMCA-generated material demonstrated that it is infectious for hamsters and maintains the distinctive strain-specific properties (Fig. 3) (16). To investigate whether PMCA can model strain interference, we added a constant amount of DY TME brain homogenate to serial 10-fold dilutions of HY TME brain homogenate and performed 10 rounds of serial PMCA. If interference did not occur in this *in vitro* system, then HY PrP<sup>Sc</sup> would be detected in the same number of PMCA rounds as PMCA reactions seeded with comparable amounts HY TME alone (Table 1). However, we found that DY TME could interfere with HY TME, as indicated by a delay in the number of rounds of PMCA required for HY PrP<sup>Sc</sup> emergence compared to PMCA reactions seeded with the same dose of HY TME alone (compare Tables 1 and 2). The number of rounds of PMCA that is required for the emergence of HY PrP<sup>Sc</sup> is dependent on the initial ratio of DY PrP<sup>Sc</sup> to HY PrP<sup>Sc</sup>, a finding consistent with *in vivo* studies (Table 2 and Fig. 4) (3, 4). This indicates that DY TME can interfere with HY TME *in vitro* similar to what is observed *in vivo* and suggests the factors that prion strains compete for is present in this system (28).

Prion strain interference is not due to DY PrP<sup>Sc</sup> converting all of the available PrP<sup>C</sup> to PrP<sup>Sc</sup>. After one round of PMCA, PrP<sup>Sc</sup> consistently accumulates to higher levels in the HY TME-seeded reactions compared to DY TME-seeded PMCA reactions (Fig. 3A and B), which is consistent with the strain-specific *in vivo* rates of PrP<sup>Sc</sup> accumulation (7, 8, 54). If DY were converting all of the available PrP<sup>C</sup> to PrP<sup>Sc</sup>, then DY and HY PrP<sup>Sc</sup> levels should be equal after one round of PMCA. Based on this observation, we hypothesize that DY PrP<sup>Sc</sup> binds to and sequesters PrP<sup>C</sup>, and/or other cofactors required for conversion, rendering it unavailable to HY PrP<sup>Sc</sup> for conversion. In other words, DY PrP<sup>Sc</sup> is occupying all of the replication sites (28). In this scenario, the excess of DY PrP<sup>Sc</sup> compared to HY PrP<sup>Sc</sup> would explain the interference effect; however, we cannot exclude the possibility that blocking strains such as DY TME have a higher affinity for PrP<sup>C</sup> compared to superinfecting short incubation period strains. Alternatively, DY PrP<sup>Sc</sup> may be competing for additional factors that affect prion replication (e.g., RNA and glycosaminoglycans) or that these factors, in combination with PrP<sup>C</sup>, form the functional replication site (18, 24, 35, 41). Studies of synthetic prion fibrils suggest that interconversion of PrP conformations occurs, therefore, interconversion of HY PrP<sup>Sc</sup> to the DY PrP<sup>Sc</sup> conformation may contribute to the interference effect (9, 51). Clearly, much work is needed to determine which of these factors are involved.

The ratio of DY TME to HY TME agent used to infect animals in our previous coinfection and superinfection studies was sufficient to allow for HY PrP<sup>Sc</sup> emergence using PMCA strain interference (Table 2) (3, 4, 8, 60). This raised the

possibility that the superinfecting prion strain can persist in coinfecting animals. To investigate this possibility, PMCA was performed on brain homogenates from animals inoculated in the sciatic nerve with the DY TME agent 120 days prior to superinfection with either the HY TME, 263K, or HaCWD agents (8, 60). These animals develop clinical signs of DY TME with no evidence of superinfecting PrP<sup>Sc</sup> by Western blot analysis (8, 60). By these criteria, DY TME had completely blocked the short incubation period superinfecting strains from causing disease. However, the addition of brain material from these animals to PMCA reactions resulted in detection of HY, 263K, or HaCWD PrP<sup>Sc</sup> after four rounds of serial PMCA (Fig. 5 and data not shown). Importantly, the detection of HY PrP<sup>Sc</sup> in the brain suggests that HY PrP<sup>Sc</sup> is transynaptically transported in the CNS. Based on these *in vitro* data, we hypothesize that HY TME would eventually emerge upon serial passage in hamsters. Overall, these data imply that in natural prion disease low levels of highly pathogenic strains may persist that could emerge upon favorable selective conditions. These conditions include serial passage, route of inoculation, or exposure of the agent to physical treatments (e.g., rendering) that would selectively destroy less-resistant strains (5, 31, 43, 64, 65).

#### ACKNOWLEDGMENTS

We thank Maria Christensen for excellent technical support and Claudio Soto for his generous advice with the PMCA reactions.

This study was supported by the National Center for Research Resources (P20 RR0115635-6, C06 RR17417-01, and G2ORR024001) and the National Institute for Neurological Disorders and Stroke (R01 NS052609).

#### REFERENCES

- Alais, S., S. Simoes, D. Baas, S. Lehmann, G. Raposo, J. L. Darlix, and P. Leblanc. 2008. Mouse neuroblastoma cells release prion infectivity associated with exosomal vesicles. *Biol. Cell* **100**:603–615.
- Ayers, J. I., A. E. Kincaid, and J. C. Bartz. 2009. Prion strain targeting independent of strain-specific neuronal tropism. *J. Virol.* **83**:81–87.
- Bartz, J. C., J. M. Aiken, and R. A. Bessen. 2004. Delay in onset of prion disease for the HY strain of transmissible mink encephalopathy as a result of prior peripheral inoculation with the replication-deficient DY strain. *J. Gen. Virol.* **85**:265–273.
- Bartz, J. C., R. A. Bessen, D. McKenzie, R. F. Marsh, and J. M. Aiken. 2000. Adaptation and selection of prion protein strain conformations following interspecies transmission of transmissible mink encephalopathy. *J. Virol.* **74**:5542–5547.
- Bartz, J. C., C. Dejoia, T. Tucker, A. E. Kincaid, and R. A. Bessen. 2005. Extraneural prion neuroinvasion without lymphoreticular system infection. *J. Virol.* **79**:11858–11863.
- Bartz, J. C., A. E. Kincaid, and R. A. Bessen. 2003. Rapid prion neuroinvasion following tongue infection. *J. Virol.* **77**:583–591.
- Bartz, J. C., A. E. Kincaid, and R. A. Bessen. 2002. Retrograde transport of transmissible mink encephalopathy within descending motor tracts. *J. Virol.* **76**:5759–5768.
- Bartz, J. C., M. L. Kramer, M. H. Sheehan, J. A. Hutter, J. I. Ayers, R. A. Bessen, and A. E. Kincaid. 2007. Prion interference is due to a reduction in strain-specific PrP<sup>Sc</sup> levels. *J. Virol.* **81**:689–697.
- Baskakov, I. V. 2009. Switching in amyloid structure within individual fibrils: implication for strain adaptation, species barrier and strain classification. *FEBS Lett.* **583**:2618–2622.
- Bessen, R. A., and R. F. Marsh. 1992. Biochemical and physical properties of the prion protein from two strains of the transmissible mink encephalopathy agent. *J. Virol.* **66**:2096–2101.
- Bessen, R. A., and R. F. Marsh. 1994. Distinct PrP properties suggest the molecular basis of strain variation in transmissible mink encephalopathy. *J. Virol.* **68**:7859–7868.
- Bessen, R. A., and R. F. Marsh. 1992. Identification of two biologically distinct strains of transmissible mink encephalopathy in hamsters. *J. Gen. Virol.* **73**:329–334.
- Bruce, M. E., I. McConnell, H. Fraser, and A. G. Dickinson. 1991. The disease characteristics of different strains of scrapie in Sinc genic mouse lines: implications for the nature of the agent and host control of pathogenesis. *J. Gen. Virol.* **72**:595–603.
- Bruce, M. E., R. G. Will, J. W. Ironside, I. McConnell, D. Drummond, A. Suttie, L. McCauley, A. Chree, J. Hope, C. Birkett, S. Cousens, H. Fraser, and C. J. Bostock. 1997. Transmissions to mice indicate that 'new variant' CJD is caused by the BSE agent. *Nature* **389**:498–501.
- Calì, I., R. Castellani, A. Alshehlee, Y. Cohen, J. Blevins, J. Yuan, J. P. Langeveld, P. Parchi, J. G. Safar, W. Q. Zou, and P. Gambetti. 2009. Co-existence of scrapie prion protein types 1 and 2 in sporadic Creutzfeldt-Jakob disease: its effect on the phenotype and prion-type characteristics. *Brain* **132**:2643–2658.
- Castilla, J., R. Morales, P. Saa, M. Barria, P. Gambetti, and C. Soto. 2008. Cell-free propagation of prion strains. *EMBO J.* **27**:2557–2566.
- Castilla, J., P. Saa, C. Hetz, and C. Soto. 2005. In vitro generation of infectious scrapie prions. *Cell* **121**:195–206.
- Caughey, B., and G. J. Raymond. 1993. Sulfated polyanion inhibition of scrapie-associated PrP accumulation in cultured cells. *J. Virol.* **67**:643–650.
- Caughey, B., G. J. Raymond, and R. A. Bessen. 1998. Strain-dependent differences in beta-sheet conformations of abnormal prion protein. *J. Biol. Chem.* **273**:32230–32235.
- Chesebro, B. 2004. Biomedicine: a fresh look at BSE. *Science* **305**:1918–1921.
- Collinge, J., M. Gorham, F. Hudson, A. Kennedy, G. Keogh, S. Pal, M. Rossor, P. Rudge, D. Siddique, M. Spyer, D. Thomas, S. Walker, T. Webb, S. Wroe, and J. Darbyshire. 2009. Safety and efficacy of quinacrine in human prion disease (PRION-1 study): a patient-preference trial. *Lancet Neurol.* **8**:334–344.
- Collinge, J., and M. Rossor. 1996. A new variant of prion disease. *Lancet* **347**:916–917.
- Collinge, J., K. C. Sidle, J. Meads, J. Ironside, and A. F. Hill. 1996. Molecular analysis of prion strain variation and the etiology of "new variant" CJD. *Nature* **383**:685–690.
- Deleault, N. R., B. T. Harris, J. R. Rees, and S. Supattapone. 2007. Formation of native prions from minimal components *in vitro*. *Proc. Natl. Acad. Sci. U. S. A.* **104**:9741–9746.
- Dickinson, A. G. 1976. Scrapie in sheep and goats. *Front. Biol.* **44**:209–241.
- Dickinson, A. G., H. Fraser, I. McConnell, G. W. Outram, D. I. Sales, and D. M. Taylor. 1975. Extraneural competition between different scrapie agents leading to loss of infectivity. *Nature* **253**:556.
- Dickinson, A. G., H. Fraser, V. M. Meikle, and G. W. Outram. 1972. Competition between different scrapie agents in mice. *Nat. New Biol.* **237**:244–245.
- Dickinson, A. G., and G. W. Outram. 1979. The scrapie replication-site hypothesis and its implications for pathogenesis, p. 13–31. *In* S. B. Prusiner and W. J. Hadlow (ed.), *Slow transmissible diseases of the central nervous system*, vol. 2. Academic Press, Inc., New York, NY.
- Ermolayev, V., T. Cathomen, J. Merk, M. Friedrich, W. Hartig, G. S. Harms, M. A. Klein, and E. Flechsig. 2009. Impaired axonal transport in motor neurons correlates with clinical prion disease. *PLoS Pathog.* **5**:e1000558.
- Ermolayev, V., M. Friedrich, R. Nozadze, T. Cathomen, M. A. Klein, G. S. Harms, and E. Flechsig. 2009. Ultramicroscopy reveals axonal transport impairments in cortical motor neurons at prion disease. *Biophys. J.* **96**:3390–3398.
- Fernie, K., P. J. Steele, D. M. Taylor, and R. A. Somerville. 2007. Comparative studies on the thermostability of five strains of transmissible-spongiform-encephalopathy agent. *Biotechnol. Appl. Biochem.* **47**:175–183.
- Fevrier, B., D. Vilette, F. Archer, D. Loew, W. Faigle, M. Vidal, H. Laude, and G. Raposo. 2004. Cells release prions in association with exosomes. *Proc. Natl. Acad. Sci. U. S. A.* **101**:9683–9688.
- Fraser, H., and A. G. Dickinson. 1967. Distribution of experimentally induced scrapie lesions in the brain. *Nature* **216**:1310–1311.
- Fraser, H., and A. G. Dickinson. 1968. The sequential development of the brain lesion of scrapie in three strains of mice. *J. Comp. Pathol.* **78**:301–311.
- Geoghegan, J. C., P. A. Valdes, N. R. Orem, N. R. Deleault, R. A. Williamson, B. T. Harris, and S. Supattapone. 2007. Selective incorporation of polyanionic molecules into hamster prions. *J. Biol. Chem.* **282**:36341–36353.
- Ghaemmaghami, S., M. Ahn, P. Lessard, K. Giles, G. Legname, S. J. DeArmond, and S. B. Prusiner. 2009. Continuous quinacrine treatment results in the formation of drug-resistant prions. *PLoS Pathog.* **5**:e1000673.
- Gousset, K., E. Schiff, C. Langevin, Z. Marjanovic, A. Caputo, D. T. Browman, N. Chenuard, F. de Chaumont, A. Martino, J. Enninga, J. C. Oliviero, D. Mannel, and C. Zurzolo. 2009. Prions hijack tunneling nanotubes for intercellular spread. *Nat. Cell Biol.* **11**:328–336.
- Gousset, K., and C. Zurzolo. 2009. Tunneling nanotubes: a highway for prion spreading? *Prion* **3**:94–98.
- Green, K. M., J. Castilla, T. S. Seward, D. L. Napier, J. E. Jewell, C. Soto, and G. C. Telling. 2008. Accelerated high fidelity prion amplification within and across prion species barriers. *PLoS Pathog.* **4**:e1000139.
- Kascsak, R. J., R. Fersko, D. Pulgiano, R. Rubenstein, and R. I. Carp. 1997. Immunodiagnosis of prion disease. *Immunol. Invest.* **26**:259–268.
- Kim, J. I., K. Surewicz, P. Gambetti, and W. K. Surewicz. 2009. The role of

- glycophosphatidylinositol anchor in the amplification of the scrapie isoform of prion protein *in vitro*. *FEBS Lett.* **583**:3671–3675.
42. **Kimberlin, R. H., S. Cole, and C. A. Walker.** 1987. Temporary and permanent modifications to a single strain of mouse scrapie on transmission to rats and hamsters. *J. Gen. Virol.* **68**:1875–1881.
  43. **Kimberlin, R. H., and C. A. Walker.** 1978. Evidence that the transmission of one source of scrapie agent to hamsters involves separation of agent strains from a mixture. *J. Gen. Virol.* **39**:487–496.
  44. **Kimberlin, R. H., C. A. Walker, and H. Fraser.** 1989. The genomic identity of different strains of mouse scrapie is expressed in hamsters and preserved on reisolation in mice. *J. Gen. Virol.* **70**:2017–2025.
  45. **Kincaid, A. E., and J. C. Bartz.** 2007. The nasal cavity is a route for prion infection in hamsters. *J. Virol.* **81**:4482–4491.
  46. **Lasmez, C. L., J. P. Deslys, R. Demaimay, K. T. Adjou, F. Lamoury, D. Dormont, O. Robain, J. Ironside, and J. J. Hauw.** 1996. BSE transmission to macaques. *Nature* **381**:743–744. (Letter.)
  47. **Legname, G., H. O. Nguyen, D. Peretz, F. E. Cohen, S. J. DeArmond, and S. B. Prusiner.** 2006. Continuum of prion protein structures enciphers a multitude of prion isolate-specified phenotypes. *Proc. Natl. Acad. Sci. U. S. A.* **103**:19105–19110.
  48. **Li, J., S. Browning, S. P. Mahal, A. M. Oelschlegel, and C. Weissmann.** 2009. Darwinian evolution of prions in cell culture. *Science* **327**:869–872.
  49. **Magalhaes, A. C., G. S. Baron, K. S. Lee, O. Steele-Mortimer, D. Dorward, M. A. Prado, and B. Caughey.** 2005. Uptake and neuritic transport of scrapie prion protein coincident with infection of neuronal cells. *J. Neurosci.* **25**:5207–5216.
  50. **Makarava, N., G. G. Kovacs, O. Bocharova, R. Savtchenko, I. Alexeeva, H. Budka, R. G. Rohwer, and I. V. Baskakov.** 2010. Recombinant prion protein induces a new transmissible prion disease in wild-type animals. 2010. *Acta Neuropathol.* **119**:177–187.
  51. **Makarava, N., V. G. Ostapchenko, R. Savtchenko, and I. V. Baskakov.** 2009. Conformational switching within individual amyloid fibrils. *J. Biol. Chem.* **284**:14386–14395.
  52. **Manuelidis, L.** 1998. Vaccination with an attenuated Creutzfeldt-Jakob disease strain prevents expression of a virulent agent. *Proc. Natl. Acad. Sci. U. S. A.* **95**:2520–2525.
  53. **Manuelidis, L., and Z. Y. Lu.** 2003. Virus-like interference in the latency and prevention of Creutzfeldt-Jakob disease. *Proc. Natl. Acad. Sci. U. S. A.* **100**:5360–5365.
  54. **Mulcahy, E. R., and R. A. Bessen.** 2004. Strain-specific kinetics of prion protein formation *in vitro* and *in vivo*. *J. Biol. Chem.* **279**:1643–1649.
  55. **Parchi, P., S. Notari, P. Weber, H. Schimmel, H. Budka, I. Ferrer, S. Haik, J. J. Hauw, M. W. Head, J. W. Ironside, L. Limido, A. Rodriguez, T. Strobel, F. Tagliavini, and H. A. Kretschmar.** 2009. Inter-laboratory assessment of PrPSc typing in Creutzfeldt-Jakob disease: a Western blot study within the NeuroPrion Consortium. *Brain Pathol.* **19**:384–391.
  56. **Peretz, D., R. A. Williamson, G. Legname, Y. Matsunaga, J. Vergara, D. R. Burton, S. J. DeArmond, S. B. Prusiner, and M. R. Scott.** 2002. A change in the conformation of prions accompanies the emergence of a new prion strain. *Neuron* **34**:921–932.
  57. **Polymenidou, M., K. Stoeck, M. Glatzel, M. Vey, A. Bellon, and A. Aguzzi.** 2005. Coexistence of multiple PrPSc types in individuals with Creutzfeldt-Jakob disease. *Lancet Neurol.* **4**:805–814.
  58. **Raymond, G. J., L. D. Raymond, K. D. Meade-White, A. G. Hughson, C. Favara, D. Gardner, E. S. Williams, M. W. Miller, R. E. Race, and B. Caughey.** 2007. Transmission and adaptation of chronic wasting disease to hamsters and transgenic mice: evidence for strains. *J. Virol.* **81**:4305–4314.
  59. **Safar, J., H. Wille, V. Itri, D. Groth, H. Serban, M. Torchia, F. E. Cohen, and S. B. Prusiner.** 1998. Eight prion strains have PrP(Sc) molecules with different conformations. *Nat. Med.* **4**:1157–1165.
  60. **Schutt, C. R., and J. C. Bartz.** 2008. Prion interference with multiple prion isolates. *Prion* **2**:61–63.
  61. **Scott, M. R., R. Will, J. Ironside, H. O. Nguyen, P. Tremblay, S. J. DeArmond, and S. B. Prusiner.** 1999. Compelling transgenic evidence for transmission of bovine spongiform encephalopathy prions to humans. *Proc. Natl. Acad. Sci. U. S. A.* **96**:15137–15142.
  62. **Sigurdson, C. J., and A. Aguzzi.** 2007. Chronic wasting disease. *Biochim. Biophys. Acta* **1772**:610–618.
  63. **Sigurdson, C. J., K. P. Nilsson, S. Hornemann, M. Heikenwalder, G. Manco, P. Schwarz, D. Ott, T. Rulicke, P. P. Liberski, C. Julius, J. Falsig, L. Stitz, K. Wuthrich, and A. Aguzzi.** 2009. De novo generation of a transmissible spongiform encephalopathy by mouse transgenesis. *Proc. Natl. Acad. Sci. U. S. A.* **106**:304–309.
  64. **Somerville, R. A., R. C. Oberthur, U. Havekost, F. MacDonald, D. M. Taylor, and A. G. Dickinson.** 2002. Characterization of thermodynamic diversity between transmissible spongiform encephalopathy agent strains and its theoretical implications. *J. Biol. Chem.* **277**:11084–11089.
  65. **Taylor, D. M., K. Fernie, I. McConnell, and P. J. Steele.** 1998. Observations on thermostable subpopulations of the unconventional agents that cause transmissible degenerative encephalopathies. *Vet. Microbiol.* **64**:33–38.
  66. **Telling, G. C., P. Parchi, S. J. DeArmond, P. Cortelli, P. Montagna, R. Gabizon, J. Mastrianni, E. Lugaresi, P. Gambetti, and S. B. Prusiner.** 1996. Evidence for the conformation of the pathologic isoform of the prion protein enciphering and propagating prion diversity. *Science* **274**:2079–2082.
  67. **Veith, N. M., H. Plattner, C. A. Stuermer, W. J. Schulz-Schaeffer, and A. Burkle.** 2009. Immunolocalization of PrPSc in scrapie-infected N2a mouse neuroblastoma cells by light and electron microscopy. *Eur. J. Cell Biol.* **88**:45–63.
  68. **Will, R. G., J. W. Ironside, M. Zeidler, S. N. Cousens, K. Estibeiro, A. Alperovitch, S. Poser, M. Pocchiari, A. Hofman, and P. G. Smith.** 1996. A new variant of Creutzfeldt-Jakob disease in the UK. *Lancet* **347**:921–925.
  69. **Wilson, M. L., and P. McBride.** 2000. Technical aspects of tracking scrapie infection in orally dosed rodents. *J. Cell. Pathol.* **5**:17–22.